Optical Materials: X 19 (2023) 100255

Contents lists available at ScienceDirect

Optical Materials: X

journal homepage: www.journals.elsevier.com/optical-materials-x

# Bismuth telluride iodide monolayer flakes with nonlinear optical response obtained via gold-assisted mechanical exfoliation

Nicolò Petrini [a,b,c,1], Aswin Asaithambi [a,1], Luca Rebecchi [a,d], Nicola Curreli [a,b,e,*]

[a] Functional Nanosystems, Italian Institute of Technology, via Morego, 30, Genova, 16163, Italy
[b] Molecular Foundry, Lawrence Berkeley National Laboratory, 67 Cyclotron Rd, Berkeley, CA, 94720, United States
[c] Dipartimento di Fisica, Università degli Studi di Genova, via Dodecaneso, 33, Genova, 16146, Italy
[d] Dipartimento di Chimica e Chimica Industriale, Università degli Studi di Genova, via Dodecaneso, 31, Genova, 16146, Italy
[e] Transport at Nanoscale Interfaces Laboratory, Empa, Swiss Federal Laboratories for Materials Science and Technology, Ueberlandstrasse 129, Dübendorf, 8600, Switzerland

ARTICLE INFO

*Keywords:*
Two-dimensional materials
Bismuth telluride iodide (BiTeI)
Gold-assisted mechanical exfoliation
Nonlinear optics
Second-harmonic generation

ABSTRACT

Bismuth telluride iodide (BiTeI) is a layered material known as Rashba semiconductor, which is promising for several applications such as spintronics, nonlinear optics, and energy-related devices. Due to its layered structure and low cleavage energy, BiTeI is particularly suitable for producing two-dimensional (2D) BiTeI crystals, allowing for the development of devices at the nanoscale. However, traditional methods of mechanically exfoliating BiTeI have encountered significant challenges. To address this, we used the so-called gold-assisted mechanical exfoliation to successfully obtain 2D BiTeI flakes. Through extensive characterization employing a range of techniques including Raman spectroscopy and second-harmonic generation (SHG) measurements, we examine the morphological, structural, and chemical properties of the gold-assisted mechanically exfoliated BiTeI flakes. We confirm their crystalline nature while also providing information about strain and defects present within the flakes. Moreover, SHG measurements revealed a significant nonlinear optical response, and the non-centrosymmetric structure observed in these flakes can be attributed to quantum confinement effects and the absence of phase-matching requirements typically found in bulk nonlinear crystals.

## 1. Introduction

In the pursuit of advancing electronic devices and pushing the boundaries of information processing, the focus has been directed towards Rashba semiconductors, a fascinating class of materials characterized by a pronounced spin-orbit coupling and associated with the Rashba effect [1,2]. These semiconductors have garnered significant interest due to their potential for revolutionizing spin-based electronics, quantum computing, and topological insulators [3]. One intriguing strategy to enable nanometer-scale spintronics operating at room temperature and facilitate nanoscale piezoelectric and nonlinear optical applications is the realization of 2D materials with giant Rashba effect [2]. Among these materials, the polar semiconductor BiTeI stands out due to its giant Rashba splitting and extraordinary electronic properties [1,4]. The polar non-centrosymmetric or non-symmorphic structure of BiTeI, coupled with its significant spin-orbit interaction effects, arises from the mixed ionic-covalent character of the compound and the presence of heavy Bi atoms [1]. These distinctive features lift the Kramer's spin degeneracy surface states, resulting in momentum-dependent spin splitting in the band structure even in the absence of an external magnetic field [5]. Ab initio calculations and angle-resolved photoemission spectroscopy studies on BiTeI have confirmed the direct consequences of the Rashba effect, such as complex Fermi surfaces and other related physical phenomena [6]. Notably, multiple-frequency Shubnikov-de Haas oscillations [7], temperature-robust Dirac Landau level structures [8], spin-polarized magneto photocurrents [9], and pressure-induced topological quantum phase transitions toward non-trivial topological insulators with material side-dependent Dirac states have been observed [7]. The evolution toward new quantum phases can lead to the fascinating pressure-dependent bulk photovoltaic effect and pressure-induced superconductivity [10]. Additionally, the unique characteristics of BiTeI,

* Corresponding author. Functional Nanosystems, Italian Institute of Technology, via Morego, 30, Genova, 16163, Italy.
*E-mail address:* nicola.curreli@iit.it (N. Curreli).
1 These authors contributed equally.

https://doi.org/10.1016/j.omx.2023.100255
Received 31 May 2023; Received in revised form 19 July 2023; Accepted 21 July 2023
Available online 28 July 2023

including the splitting of surface states from the bulk bands and the ability to control spin information through modulation of chemical potential, doping, or mechanical stress, have the potential to revolutionize energy-related devices [4,11]. The possibility of generating free carriers in BiTeI monolayers through energy transfer presents exciting opportunities for the development of electrocatalytic systems [12]. This potential is also observed in other bismuth-containing materials, which exhibit energy conversion and harvesting properties [13,14]. Consequently, this breakthrough could lead to innovative approaches in areas such as photovoltaics, photoelectrochemical cells, and other energy conversion devices, where precise control and manipulation of free carriers play a crucial role in enhancing overall performance, as also demonstrated in other 2D materials [11,15,16]. In this context, pioneering and recent theoretical studies coupled with experimental observations have revealed that BiTeI exhibits a giant Rashba spin splitting of approximately 400 meV, which is among the largest reported to date [5]. The layered structure of BiTeI, consisting of ionically bound $(BiTe)^+$ and $I^-$ layers, forms BiTeI trilayers held together by van der Waals forces [17]. Consequently, the plane between Te and I serves as a natural cleavage plane of the crystal, leading to Te- or I-terminated surfaces [17]. With the rapid advances in designing artificial van der Waals heterostructures by stacking 2D materials, exfoliated BiTeI flakes hold potential as architectural components in functional quantum systems, including the realization of time-reversal invariant topological insulating phases such as the predicted $Bi_2Te_2I_2$ sextuple layer composed of Te-faced BiTeI [18]. However, despite the layered structure of bulk BiTeI and the predicted low cleavage energy required to obtain its monolayer, the exfoliation of BiTeI into single- or few-layer forms remains challenging. Approaches using electrochemical [12], and liquid phase exfoliation [4] have shown a lack of control over the thickness, resulting in films of BiTeI flakes having thicknesses ranging from monolayer to > 100 nm crystals for the exfoliated flakes. This lack of uniformity hampers the study of the electronic band structure of BiTeI and restricts the design and fabrication of devices with consistent and predictable performance characteristics. Furthermore, the optical properties of BiTeI are intricately linked to its thickness, and uncontrolled thickness distribution in flakes impedes accurate interpretation of experimental results and limits the exploitation of specific optical phenomena [4]. In another study [3], BiTeI monolayers were obtained by mechanically exfoliating the flakes onto an Au substrate. However, this methodology led to strong hybridization between the BiTeI monolayer and the Au substrate, altering the charge distribution on the BiTeI surface, resulting in substantial modifications of the electronic band structure and optical properties of the material [3].

In our work, we have successfully addressed these challenges by employing a gold-assisted mechanical exfoliation method that takes advantage of the strong affinity between BiTeI and gold, while allowing the transfer of the exfoliated flake onto a silicon substrate. This enables comprehensive investigation of the optical properties of BiTeI in the monolayer form, by achieving precise control over the thickness of the obtained monolayers. The structural and optical properties of monolayer BiTeI flakes were evaluated in this study using Raman spectroscopy and second-harmonic generation (SHG). The concurrent presence of spin-orbit coupling and structural inversion asymmetry in Rashba-type materials gives rise to nonlinear optical signals. The absence of inversion symmetry and strong quantum confinement in these materials can lead to extraordinary second-order nonlinear optical effects. Additionally, the nanometric thickness of exfoliated materials allows them to bypass phase-matching constraints encountered in three-dimensional nonlinear crystals, as the coherence length of the second-harmonic is much larger than the thickness of the 2D materials. As a result, the measurement of SHG from few-layer BiTeI flakes reveals a significant nonlinear optical response. Consequently, 2D Rashba-type BiTeI offers a novel nanometer-thin platform for studying nonlinear optical phenomena.

## 2. Materials and methods

### 2.1. Gold-assisted mechanical exfoliation

The BiTeI bulk crystal was purchased from HQ Graphene, the Netherlands, with a crystal size of up to 1 mm. As reported in Ref. [19], a 150 nm thick layer of gold is deposited onto a silicon substrate with 285 nm thermal oxide using sputter coater KS500 Confocal, Kenosistec. A solution of polyvinylpyrrolidone (PVP) was then spin-coated onto the gold film, followed by curing at 150 °C for 5 min to serve as a sacrificial layer, preventing contamination from tape residue. The PVP-coated gold film was applied gently onto a freshly cleaved bulk BiTeI crystal using thermal release tape, which could be removed at a temperature of 90 °C. This process allowed the monolayer 2D crystal attached to the gold surface to transfer onto a $Si/SiO_2$ substrate.

It is important to note that the adhesion between gold and $Si/SiO_2$ surfaces is weak due to the difference in their surface energies [20,21]. This difference in surface properties hinders direct adhesion between gold and $Si/SiO_2$. To overcome this issue, surface functionalization is employed to modify the properties of the $Si/SiO_2$ substrate. We used (3-Aminopropyl) triethoxysilane (APTES) as a surface functionalization agent. APTES promotes chemical bonding between the amino groups of APTES and the hydroxyl groups on the $Si/SiO_2$ surface, thereby improving the adhesion between the two materials. APTES was prepared using atomic layer deposition (ALD). The $Si/SiO_2$ substrate was placed inside the ALD chamber, which was purged with nitrogen gas. Subsequently, the APTES precursor was introduced into the ALD chamber. The APTES deposition was carried out at a temperature of 110 °C. The precursor was pulsed into the chamber, allowing it to react with the substrate surface. The specific deposition conditions, such as pressure, pulse duration, and purge duration, were optimized for APTES growth at this temperature.

The thermal release tape was subsequently removed by heating at 130 °C. The PVP layer was dissolved in deionized (DI) water for 2 h. The sample, covered with the gold layer, was rinsed with acetone and cleaned with $O_2$ plasma for 3 min to eliminate any remaining polymer residues. Eventually, the gold layer was dissolved using a $KI/I_2$ Au etchant solution composed of 2.5 g $I_2$ and 10 g KI in 100 ml DI water. The resulting monolayer was then rinsed with DI water and isopropanol, and dried using $N_2$.

### 2.2. Material characterization

Scanning electron microscopy (SEM) and energy-dispersive X-ray spectroscopy (EDX) measurements on the BiTeI flakes were performed using a Helios Nanolab 600 instrument from FEI Company along with an X-Max detector and INCA s system from Oxford Instruments for the acquisition and analysis of EDX spectra. The SEM measurements employed a 20 kV accelerating voltage and a beam current of 0.2 nA. The EDX measurement values were adjusted to 20 kV and 0.8 nA. The sample was imaged without the application of any conductive coating on the surface.

Atomic force microscopy (AFM) images were acquired using an XE-100 AFM system from Park System, Korea. PPP-NCHR probes from Nanosensors, USA, with a nominal tip diameter of less than 10 nm and a drive frequency of approximately 330 kHz were used. Non-contact mode AFM images consisting of 512 × 512 data points were collected for areas of 25 × 25 $\mu m^2$. The working setpoint was maintained above 65% of the free oscillation amplitude. The scan rate for image acquisition was set to 0.2 Hz. Height profiles were processed using Gwyddion software.

Raman spectroscopy measurements were conducted using a Renishaw micro-Raman InVia system equipped with a 100 × objective. The excitation wavelength employed was 514.5 nm, with a time exposure of 1 s, and the incident power was set at 1 mW.

Nonlinear optical measurements are performed on BiTeI flakes exfoliated onto a $Si/SiO_2$ substrate. The optical excitation is provided with an 80 MHz pulsed Chameleon OPO laser with tunable wavelength (OPO: 1070–1340 nm, fundamental: 680–1080 nm). The excitation wavelength used in the SHG measurement was 1200 nm. The excitation laser was coupled into IX83 Olympus microscope via a 1000 nm short-pass dichroic (DMSP1000R) and focused on the sample (BiTeI) with a 40 × (N.A. 0.5) reflective objective (LMM40X-P01). The SHG light was collected by the same reflective objective, which was used for detection. The SHG light was filtered for the fundamental using a dichroic short-pass filter (DMSP1000R) and focused on the slit of a Czerny-Turner HRS-500 spectrometer (Princeton Instruments) to resolve the light spectrally. The spectrally resolved light was detected and read using a PIXIS CCD camera and Lightfield software (Princeton Instruments). The 2nd order noise of the fundamental from the grating was checked by collecting a spectrum from a reflecting surface.

## 3. Results

Hexagonal crystals of BiTeI (space group P3m1, no. 156) have been exfoliated by gold-assisted mechanical exfoliation, as detailed in Section 2. The inset in the crystal photograph, depicted in Fig. 1a, showcases its layered structure consisting of ionically bonded $(BiTe)^{+}$ and $I^{-}$ layers. These layers form trilayers with I–Bi–Te stacking, interlinked by van der Waals forces. Based on the calculated cleavage energy required to obtain its monolayer (approximately 90 meV/atom [22]) by cleaving the crystals along the Te–I plane, we explored the exfoliation of bulk BiTeI crystals using the gold-assisted exfoliation method. The resulting flakes primarily exhibit monolayer crystals, but some bulk BiTeI crystals remained after exfoliation. The contour of the BiTeI flakes is clearly discernible in bare optical microscopy images, as exemplified in Fig. 1a. However, the presence of wrinkled regions within the flakes indicates the occurrence of discontinuities attributable to the forces experienced during exfoliation. These localized structural variations within the monolayer flakes could influence the material's properties.

To further examine the flakes, we performed atomic force microscopy (AFM) measurements on the selected sample. Fig. 1b shows an AFM image of the analyzed flake as depicted in Fig. 1a. By measuring step heights at various positions, and employing different PID control parameters, we obtained step heights in the range of approximately 1.3 nm. This value closely aligns with the bulk lattice parameters of BiTeI in the out-of-plane direction, which have been reported as 6.5 Å [23] and 6.8 Å [24], as well as to the measured thickness of the BiTeI flake in a prior investigation conducted on an Au substrate (8.5 Å [3]). Therefore, we conclude that the measured step height corresponds to a single-layer crystal of BiTeI. It is worth noting that this slight discrepancy could be attributed to the fact that height measurements on different substrates may deviate by a few Angstroms in AFM profiles [25]. We further investigated the wrinkles present on the flake, which manifest as folds in the surface morphology. Height variations associated with these wrinkles were measured, yielding values ranging from 1 nm to 3 nm. These measurements indicate the presence of substantial structural deformations on the surface of the BiTeI flake. The observed wrinkles are likely a consequence of strain or stress relaxation processes that occur during the exfoliation and transfer of the flake onto the substrate. Based on our findings, monolayer BiTeI can indeed be obtained through the gold-assisted mechanical exfoliation technique, thereby showcasing its potential as a robust method for producing large-size 2D crystals beyond graphene and transition metal dichalcogenides.

The structural properties of the BiTeI flakes were evaluated using Raman spectroscopy. Fig. 1c illustrates the Raman spectra of both the BiTeI flakes and bulk crystals. Group theory predicts four active Raman modes with the irreducible vibrational representation $\Gamma = 2A_1 + 2E$ (i.e., two E modes and two $A_1$ modes) [26]. In contrast to previous studies on monolayer BiTeI, the presence of distinct Raman peaks in our exfoliated sample indicates the high crystallinity of the BiTeI flakes [3,12]. Compared to the bulk crystal, the monolayer counterpart exhibits peaks at 90 and 147 $cm^{-1}$, assigned to $A_1(1)$ and $A_1(2)$ modes, respectively, while E(1) and E(2) are observed at 51 and 100 $cm^{-1}$. It is worth noting that the $A_1(1)$ peak in the bulk is redshifted compared to the $A_1(1)$ peak in the monolayer, whereas the $A_1(2)$ peak in the bulk is blueshifted compared to the $A_1(2)$ peak in the monolayer. This suggests the potential involvement of several phenomena, including stress or strain effects, which can affect the crystalline structure and molecular vibrations, interatomic interactions, and quantum confinement effect, influencing molecular vibrations, as well as changes in the interlayer interaction strength. In addition, the presence of wrinkles and folds in the monolayer introduces local perturbations in the material's structure, which influence the Raman response. The increase in peak intensities and the slight redshift observed in $A_1(1)$ peak can be attributed to these strain-induced displacements, as also demonstrated for other 2D materials [27].

Additionally, Fig. 2a displays a SEM image of exfoliated BiTeI crystal. The SEM-coupled energy-dispersive X-ray spectroscopy analysis, as depicted in Fig. 2b–d, show that the exfoliated BiTeI crystals have a non-ideal stoichiometry with ratios of 0.86:1:0.89 for Bi, Te, and I, respectively. These deviations in stoichiometry can indicate local variations in the crystal phase of the exfoliated material, thereby affecting the crystal structure and leading to shifts in the frequencies of molecular vibrations, as reflected also by the Raman analysis. It is worth noting that the Bi, Te

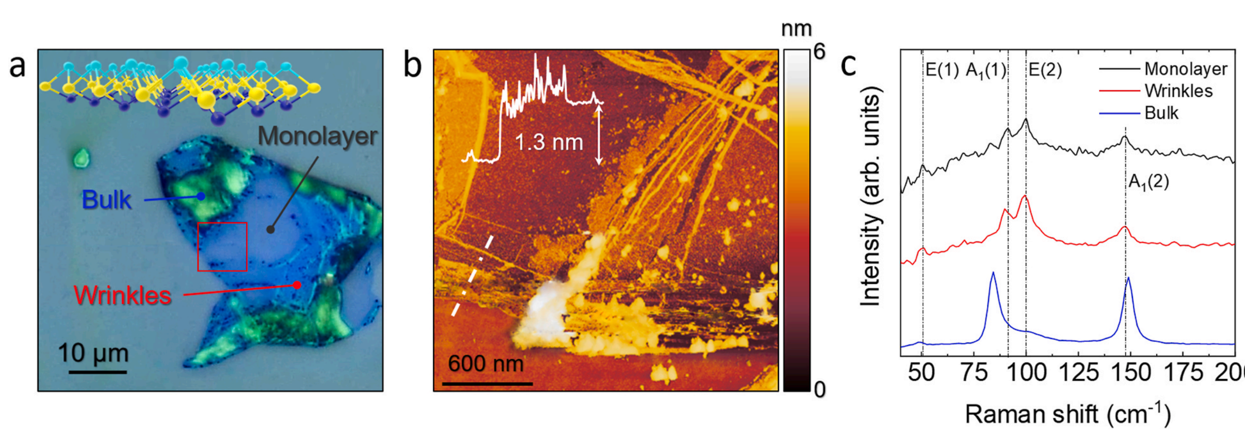


**Fig. 1.** a) Optical micrograph of an exfoliated monolayer BiTeI crystal produced via gold-assisted mechanical exfoliation. The crystal structure (space group P3m1, no. 156) of the BiTeI crystals is also depicted in the inset. The red box indicates the region considered for atomic force microscopy measurements in b. b) Atomic Force Microscopy image of a monolayer BiTeI flake. The dashed white line represents the flake thickness profile (inset). c) Raman spectra (excitation wavelength of 514 nm) of BiTeI bulk crystal, monolayer, and wrinkles. The panel displays the Raman modes associated with the hexagonal P3m1 structure of the BiTeI crystals. (For interpretation of the references to colour in this figure legend, the reader is referred to the Web version of this article.)

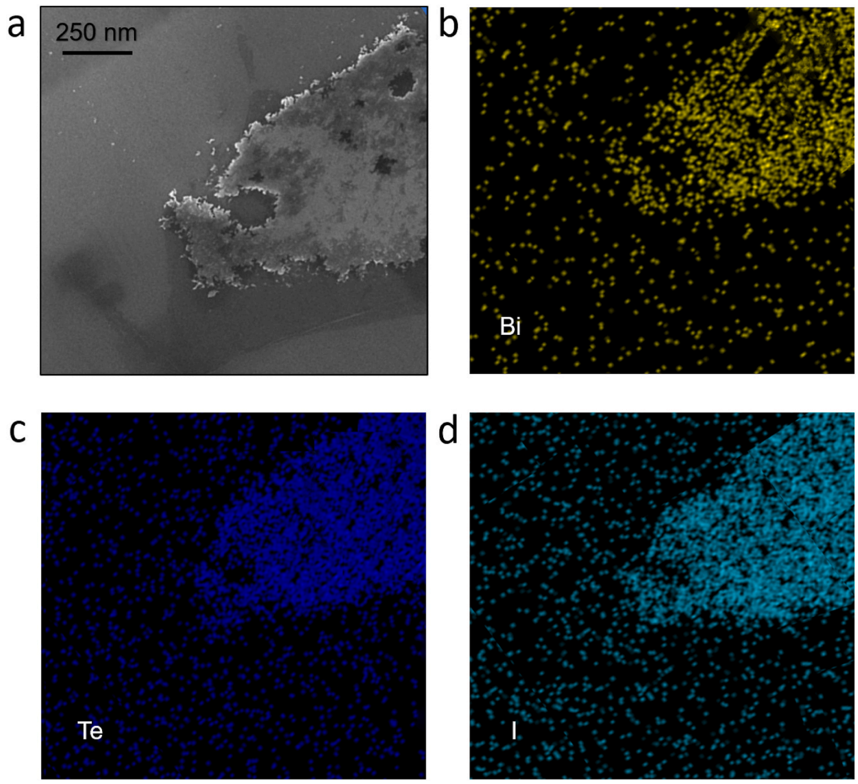


**Fig. 2.** a) SEM image of a BiTeI flake and the corresponding quantitative SEM-EDX maps of b) Bi (L$\alpha$1 line), c) Te (L$\alpha$1 line), and d) I (L$\alpha$1 line), respectively.

and I EDX signal is clearly present in the bulk region, whereas the high accelerating voltage required for signal collection decreases the probability of interaction between high accelerated electrons and the surface, thus preventing any signal from the monolayer region.

BiTeI crystals, which possess intrinsically broken inversion symmetry, exhibit ultrastrong, nonlinear susceptibilities, as evidenced by their intense SHG. Hence, to verify the crystalline quality and non-centrosymmetric structure of BiTeI crystals, we assess their nonlinear optical properties using SHG. Fig. 3 illustrates the emission of SH light from BiTeI flakes obtained through gold-assisted mechanical exfoliation, which are deposited onto a $Si/SiO_2$ substrate. The excitation is performed using pulsed light at the 1200 nm wavelength. The absence of a phase-matching requirement at sub-wavelength thicknesses implies that the nonlinear conversion efficiency reported below does not exhibit strong dispersion, allowing for broadband operation. Considering the absence of an SH response from the $Si/SiO_2$ substrate, the experimental results demonstrate that the BiTeI flake exhibits a nonlinear response in both the monolayer and bulk counterparts (Fig. 3a). Despite the absence of discernible data within the monolayer region on the SHG map, it is important to note that the signal-to-noise ratio is notably low in these specific regions (Fig. 3a). This is attributed to the limited integration time for mapping, which was set to 3 s. However, upon analyzing individual spectra obtained from the monolayer with an extended integration time of 10 s, a more pronounced signal-to-noise ratio is observed, and the signal becomes clearly detectable (Fig. 3b). In monolayer BiTeI, SHG response is primarily influenced by the constructive interference of adjacent layers. This coherent enhancement is made possible by the negligible phase mismatch that occurs over nanometer distances. As expected, the bulk material demonstrates a significantly larger nonlinear response, surpassing the monolayer response by more than one order of magnitude. Therefore, as the lattice thickness increases, the coherent response continues to increase, as illustrated in Fig. 3b. Second-order nonlinear susceptibility $\chi^{(2)}$ is proportional to the square root of the detected power of the SHG ($P_{det}$), inversely proportional to the power of the fundamental light ($I(\omega)$) and the volume of the crystal (V) as shown in Equation (1) [4]:

$$\chi^{(2)} \sim \frac{\sqrt{P_{det}}}{I(\omega)\cdot V} \tag{1}$$

Considering the volume of bulk is 100 fold more than the monolayer gathered from the height profile of the AFM data, $\chi^{(2)}$ of the monolayer is at least 11 fold more than the bulk which is consistent with the literature [4].

## 4. Conclusions

To summarize, we present a method for the exfoliation of monolayer BiTeI single crystals, which serve as a model for layered Rashba-type materials. We assessed their morphological, structural, optical, and chemical characteristics using a combination of microscopic and spectroscopic techniques, demonstrating that the gold-assisted mechanical exfoliation of monolayer BiTeI crystals maintains their crystalline integrity, as confirmed by AFM imaging and Raman characterization. Furthermore, the non-centrosymmetric structure and crystallinity of both bulk and exfoliated BiTeI were confirmed through their nonlinear optical response. In this work, we also demonstrated the nonlinear frequency up-conversion of NIR light, which has significant technological relevance as it enables detection using silicon-based devices. This highlights the potential of monolayer BiTeI for advanced solution-processed applications, including spin(orbi)tronic, thermoelectric, piezoelectric, and nonlinear optical systems, as well as other energy conversion devices.

## CRediT authorship contribution statement

**Nicolò Petrini:** Investigation, Writing – review & editing. **Aswin Asaithambi:** Investigation, Writing – review & editing. **Luca Rebecchi:** Investigation, Writing – review & editing. **Nicola Curreli:** Conceptualization, Investigation, Methodology, Validation, Formal analysis,

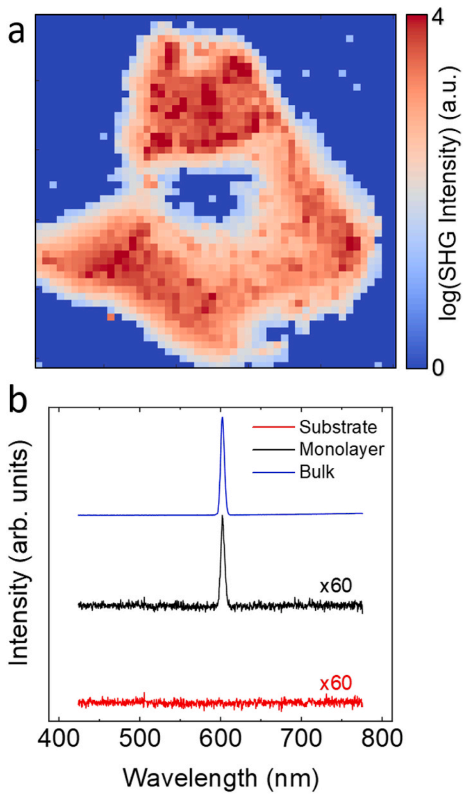


**Fig. 3.** a) Second Harmonic Generation (SHG) intensity mapping for the BiTeI sample, with an integration time of 3s and power set at 2 mW. b) SHG spectral intensity for substrate, monolayer flake, and bulk, respectively, with an integration time of 10s and power set at 2 mW. The intensities of the substrate and monolayer spectra were scaled up by a factor of 60 for better comparison with the bulk spectrum.

Writing – original draft, Writing – review & editing, Visualization, Supervision.

## Declaration of competing interest

The authors declare that they have no known competing financial interests or personal relationships that could have appeared to influence the work reported in this paper.

## Data availability

Data will be made available on request.

## Acknowledgements

For this work, the authors received financial support of both the European Union's Horizon 2020 Research and Innovation programme under grant agreement no. 101017821 (LIGHT-CAP FET proactive project), the European Union's Horizon 2020 European Research Council under grant agreement no. 850875 (Light-DYNAMO project) and the Horizon Europe European Research Council Proof of Concept under grant agreement no. 101069295 (CONDINKS project). N.C. acknowledges the European Commission for the Marie Curie Global Fellowship under grant agreement no. 101109662 (2DTWIST).

## References

[1] M.S. Bahramy, R. Arita, N. Nagaosa, Origin of giant bulk Rashba splitting: application to BiTeI, Phys. Rev. B 84 (4) (2011), 041202.
[2] Seungjun Lee, Young-Kyun Kwon, Unveiling giant hidden Rashba effects in two-dimensional $Si_2Bi_2$, npj 2D Mater. Appl. 4 (1) (2020) 45.
[3] Bálint Fülöp, Zoltán Tajkov, János Pető, Péter Kun, János Koltai, László Oroszlány, Endre Tóvári, Hiroshi Murakawa, Yoshinori Tokura, Sándor Bordács, et al., Exfoliation of single layer BiTeI flakes, 2D Mater. 5 (3) (2018), 031013.
[4] Gabriele Bianca, Chiara Trovatello, Attilio Zilli, Marilena Isabella Zappia, Sebastiano Bellani, Nicola Curreli, Irene Conticello, Joka Buha, Marco Piccinni, Michele Ghini, et al., Liquid-phase exfoliation of bismuth telluride iodide (BiTeI): structural and optical properties of single-/few-layer flakes, ACS Appl. Mater. Interfaces 14 (30) (2022) 34963–34974.
[5] K. Ishizaka, M.S. Bahramy, H. Murakawa, M. Sakano, T. Shimojima, T. Sonobe, K. Koizumi, S. Shin, H. Miyahara, A. Kimura, et al., Giant Rashba-type spin splitting in bulk BiTeI, Nat. Mater. 10 (7) (2011) 521–526.
[6] Gabriel Landolt, Sergey V. Eremeev, Yury M. Koroteev, Bartosz Slomski, Stefan Muff, Titus Neupert, Masaki Kobayashi, Vladimir N. Strocov, Thorsten Schmitt, Ziya S. Aliev, et al., Disentanglement of surface and bulk Rashba spin splittings in noncentrosymmetric BiTeI, Phys. Rev. Lett. 109 (11) (2012), 116403.
[7] T. Ideue, J.G. Checkelsky, M.S. Bahramy, H. Murakawa, Y. Kaneko, N. Nagaosa, Y. Tokura, Pressure variation of Rashba spin splitting toward topological transition in the polar semiconductor BiTeI, Phys. Rev. B 90 (16) (2014), 161107.
[8] Sándor Bordács, Joseph G. Checkelsky, Hiroshi Murakawa, Harold Y. Hwang, Yoshinori Tokura, Landau level spectroscopy of Dirac electrons in a polar semiconductor with giant Rashba spin splitting, Phys. Rev. Lett. 111 (16) (2013), 166403.
[9] N. Ogawa, M.S. Bahramy, H. Murakawa, Y. Kaneko, Y. Tokura, Magnetophotocurrent in BiTeI with Rashba spin-split bands, Phys. Rev. B 88 (3) (2013), 035130.
[10] Yanpeng Qi, Wujun Shi, Pavel G. Naumov, Nitesh Kumar, Raman Sankar, Walter Schnelle, Shekhar Chandra, Fang-Cheng Chou, Claudia Felser, Binghai Yan, et al., Topological quantum phase transition and superconductivity induced by pressure in the bismuth tellurohalide BiTeI, Adv. Mater. 29 (18) (2017), 1605965.
[11] Dimitris Tsikritzis, Konstantinos Chatzimanolis, Nikolaos Tzoganakis, Sebastiano Bellani, Marilena Isabella Zappia, Gabriele Bianca, Nicola Curreli, Joka Buha, Ilka Kriegel, Nikolas Antonatos, et al., Two-dimensional BiTeI as a novel perovskite additive for printable perovskite solar cells, Sustain. Energy Fuels 6 (23) (2022) 5345–5359.
[12] Nikolas Antonatos, Evgeniya Kovalska, Vlastimil Mazanek, Vesely Martin, David Sedmidubsky, Bing Wu, Zdenek Sofer, Electrochemical exfoliation of Janus-like BiTeI nanosheets for electrocatalytic nitrogen reduction, ACS Appl. Nano Mater. 4 (1) (2021) 590–599.
[13] Mengjiao Wang, Silvio Osella, Rosaria Brescia, Zheming Liu, Jaime Gallego, Mattia Cattelan, Matteo Crisci, Stefano Agnoli, Teresa Gatti, 2D $MoS_2$/BiOBr van der Waals heterojunctions by liquid-phase exfoliation as photoelectrocatalysts for hydrogen evolution, Nanoscale 15 (2) (2023) 522–531.
[14] Mengjiao Wang, Matteo Crisci, Matilde Pavan, Zheming Liu, Jaime Gallego, Teresa Gatti, New insights into the surfactant-assisted liquid-phase exfoliation of $Bi_2S_3$ for electrocatalytic applications, Catalysts 13 (3) (2023) 551.
[15] Aswin Asaithambi, Nastaran Kazemi Tofighi, Nicola Curreli, Manuela De Franco, Aniket Patra, Nicolò Petrini, Dmitry Baranov, Liberato Manna, Francesco Di Stasio, Ilka Kriegel, Generation of free carriers in $MoSe_2$ monolayers via energy transfer from $CsPbBr_3$ nanocrystals, Adv. Opt. Mater. 10 (14) (2022), 2200638.
[16] Gabriele Bianca, Marilena Isabella Zappia, Sebastiano Bellani, Michele Ghini, Nicola Curreli, Joka Buha, Valerio Galli, Mirko Prato, Aljoscha Soll, Zdeněk Sofer, et al., Indium selenide/indium tin oxide hybrid films for solution-processed photoelectrochemical-type photodetectors in aqueous media, Adv. Mater. Interfac. 10 (1) (2023), 2201635.
[17] A.V. Shevelkov, E.V. Dikarev, R.V. Shpanchenko, B.A. Popovkin, Crystal structures of bismuth tellurohalides BiTeX (X = Cl, Br, I) from X-ray powder diffraction data, J. Solid State Chem. 114 (2) (1995) 379–384.
[18] I.A. Nechaev, S.V. Eremeev, E.E. Krasovskii, Pedro M. Echenique, Eugene V. Chulkov, Quantum spin Hall insulators in centrosymmetric thin films composed from topologically trivial BiTeI trilayers, Sci. Rep. 7 (1) (2017) 1–8.
[19] Fang Liu, Wenjing Wu, Yusong Bai, Sang Hoon Chae, Qiuyang Li, Jue Wang, James Hone, X.-Y. Zhu, Disassembling 2D van der Waals crystals into macroscopic monolayers and reassembling into artificial lattices, Science 367 (6480) (2020) 903–906.
[20] P. Benjamin, C. Weaver, The adhesion of evaporated metal films on glass, Proc. Roy. Soc. Lond. Math. Phys. Sci. 261 (1307) (1962) 516–531.
[21] Emily A. Weiss, George K. Kaufman, Jennah K. Kriebel, Zhefeng Li, Richard Schalek, George M. Whitesides, Si/$SiO_2$-templated formation of ultraflat metal surfaces on glass, polymer, and solder supports: their use as substrates for self-assembled monolayers, Langmuir 23 (19) (2007) 9686–9694.
[22] Torbjörn Björkman, Andris Gulans, Arkady V. Krasheninnikov, Risto M. Nieminen, van der Waals bonding in layered compounds from advanced density-functional first-principles calculations, Phys. Rev. Lett. 108 (23) (2012), 235502.
[23] Vladimir A. Kulbachinskii, Vladimir G. Kytin, Alexey A. Kudryashov, Alexei N. Kuznetsov, Andrei V. Shevelkov, On the electronic structure and thermoelectric properties of BiTeBr and BiTeI single crystals and of BiTeI with the addition of $BiI_3$ and CuI, J. Solid State Chem. 193 (2012) 154–160.
[24] R. Sankar, I Panneer Muthuselvam, Christopher John Butler, S.-C. Liou, B.H. Chen, M.-W. Chu, W.L. Lee, Minn-Tsong Lin, R. Jayavel, F.C. Chou, Room temperature agglomeration for the growth of BiTeI single crystals with a giant Rashba effect, CrystEngComm 16 (37) (2014) 8678–8683.

[25] P. Nemes-Incze, Z. Osváth, K. Kamarás, L.P. Biró, Anomalies in thickness measurements of graphene and few layer graphite crystals by tapping mode atomic force microscopy, Carbon 46 (11) (2008) 1435–1442.
[26] I. Yu Sklyadneva, R. Heid, K.-P. Bohnen, V. Chis, V.A. Volodin, K.A. Kokh, O. E. Tereshchenko, P.M. Echenique, E.V. Chulkov, Lattice dynamics of bismuth tellurohalides, Phys. Rev. B 86 (9) (2012), 094302.
[27] Shengxue Yang, Yujia Chen, Chengbao Jiang, Strain engineering of two-dimensional materials: methods, properties, and applications, InfoMat 3 (4) (2021) 397–420.